

# Geo-matching with simultaneous altitude measurement for SAR-aided navigation systems

M. Wielgo, K. Abratkiewicz, D. Gromek, P. Samczyński, K. Stasiak  
POLAND

m.wielgo@elka.pw.edu.pl, d.gromek@elka.pw.edu.pl

## **ABSTRACT**

*In many civil and military UAVs applications, precise trajectory estimation and correction are crucial for mission success. Most commonly used navigational systems are based on satellite radionavigation and inertial navigation systems (INS). These solutions, however, are not always reliable. The availability of the global navigation satellite systems (GNSS) may cease for several reasons, especially if we do not control them. Another reason why the GNSS may be unavailable or provide incorrect information is electronic warfare, in particular jamming and spoofing. The latter can even be used to alter the UAV's trajectory leading to its destruction. On the other hand, the INS platforms are known for their long-time drift, which creates the need for the use of precise and expensive fiber-optic (or laser) gyroscopes and periodic recalibration. The recalibration is also problematic if the flight model is complicated, as when we consider modern multi-propeller drones or other highly manoeuvring platforms. This paper presents an algorithm of cumulative minimum square distance matching with simultaneous altitude measurement for SAR-aided navigation systems. The algorithm needs only one radar sensor and allows for cyclic trajectory parameters estimation based on optical and SAR image matching with simultaneous altitude measurement.*

## **1.0 INTRODUCTION**

Nowadays, most aerial vehicles are steered and supported by few different navigation systems. The use of at least two different navigation systems on one platform has become particularly important for several reasons. Firstly, the aim is to increase the precision of ammunition and flying objects. Secondly, it is necessary to create systems that can work without the support of GNSS (Global Navigation Satellite System). The GNSS signals are globally available; however, in the case of international military conflicts, these signals might be easily interrupted or jammed. In cases of absence of a satellite signal, it is necessary to create independent systems that still allow for precise navigation. The most commonly used additional sensor that allows the navigation of objects is the inertial navigation system (INS). Nevertheless, due to the significant drift of the IMU sensors in INS, inertial navigation still requires additional systems. One solution to support the INS that can be found on the market is based on additional sensors that measure an actual platform i.e radar altimeter or LIDAR. The range profile gathered during flight is then correlated with the digital elevation model (DEM) database stored in the system. Such systems are called Terrain Contour Matching (TERCOM) [1]-[3] and are often used to support navigation of UAVs or cruise missiles in an environment where jamming of GNSS systems is suspected.

Instead of using the one-dimensional TERCOM technique, there are also known Digitized Scene-Mapping Area Correlators (DSMAC)[4]-[6], which could guide missiles in real-time by using camera inputs to determine their location. Such a system works by comparing camera inputs during flight to maps stored from satellite images. Since the data are not identical and would change with the seasons and from other unexpected changes and visual effects, the DSMAC system within the missiles would have to compare and determine if the maps were the same, regardless of changes. By this method, it could successfully filter out differences in maps and use the remaining map data to determine its location. Such a system is, however, sensitive to weather conditions. DSMAC systems are often combined with TERCOM as a terminal guidance

system, allowing precise navigation at the final stage.

The latest developments which can be found in the literature are focused on the use of Synthetic Aperture Radar (SAR) and Interferometric SAR (InSAR) radar for navigation correction [4]–[7]. Unlike optical images, SAR/InSAR images can be easily applied to help navigation systems in all-weather conditions – cloud cover, night, rain. In such cases, the navigation subsystem is equipped with a SAR radar sensor and a database with georeferenced optical images on board the flying platform. During the flight, the terrain is scanned by the radar, and the obtained SAR image is compared to the corresponding optical one in the database, and the inertial navigation error can be reduced.

Such a concept of utilizing SAR and InSAR sensors to support onboard air platform navigational devices was proposed several years ago in the SARINA (SAR-based Augmented Integrity Navigation Architecture) project [7]–[10], where the authors were involved. That project was at the conceptual stage (technical readiness level (TRL) 3–4), but it proved that SAR/InSAR sensors could be successfully used to support navigational devices. In the SARINA project, the merging of simulated SAR/InSAR images with an optical image database was based on simple automatic shape recognition of the terrain targets, using target contours extraction. Image processing was then applied (including different techniques, such as the Hough transform) to find targets and recognize their shape. These techniques were used for SAR image matches. Also, for InSAR, algorithms based on matching 3D SAR interferograms with LIDAR elevation models were developed.

The auspicious results of the previous SARINA project motivated the authors to continue work on the topic and start developing a system on a higher TRL level. In the meantime, new SAR and optical image processing algorithms have been developed in other fields, such as geodesy. The authors intend to test the efficiency of these techniques and assess their usability for air platform navigation. One such approach is based on the scale-invariant feature transform (SIFT) technique and was presented by the authors in [7]. The novelty and application of this approach is presented in [8]. The SIFT/Affine-SIFT (ASIFT) algorithm was used to find and match corresponding keypoints appearing in the SAR and optical images. Based on previous experiments and simulations with ASIFT algorithm, authors have proposed a novel approach utilizing the more robust CMSD (Cumulative Minimum Square Distance) method and its limitations. The novelty of the solution proposed and described in this paper is the utilization of an innovative approach to the shift and rotation estimation between the SAR and optical images.

This paper focuses on finding characteristic points in both images SAR and ortophotomap by applying the classical Sobel edge detection algorithm. Before finding characteristic points in each image, additional preprocessing on SAR and ORTO images is needed. To the author's best knowledge, an innovative approach to the shift and rotation estimation between SAR and optical images by applying CMSDM technique on detected pixels has not been used for navigation drift correction on a flying platform similar to the one considered in this paper. In the following part, the authors present an overview of the CMSDM technique – its modifications and the required preprocessing – and its limits, which is taken into account when developing systems based on SAR systems for navigation drift corrections.

## **1.0 SYSTEM ARCHITECTURE**

In this chapter, an architecture of the navigation aid system concept is presented. As it can be seen in Figure 1-1, the system has two main parts:

- Mission Planner & Digital Image Processing Ground Station
- Airborne navigation SAR-aided system

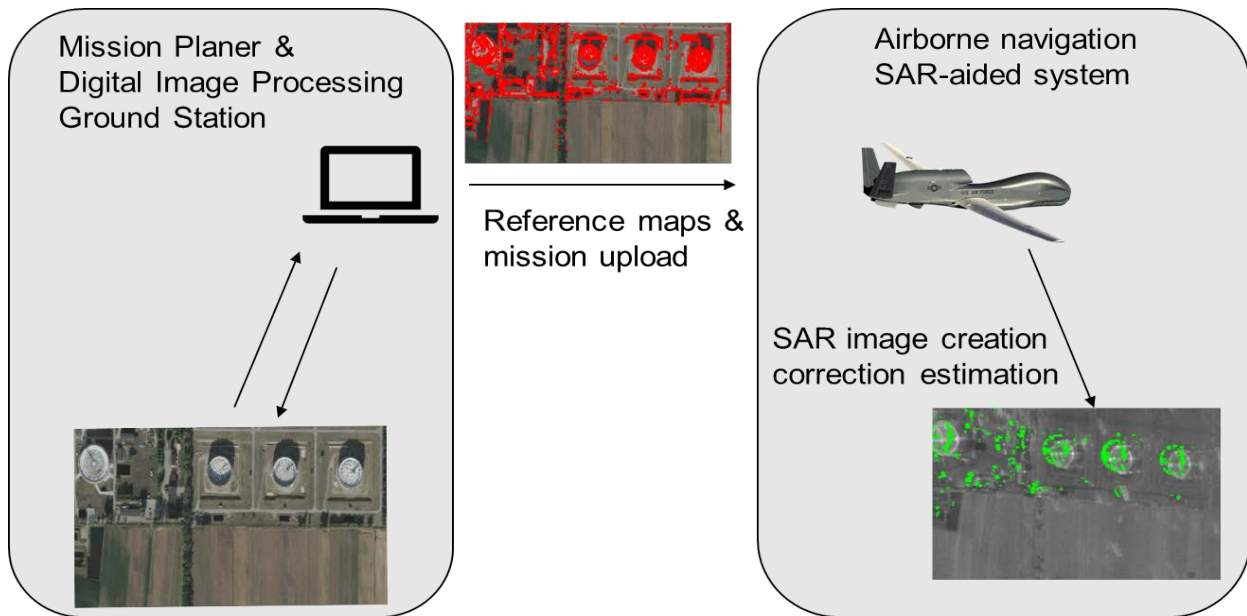


**Figure 1-1: System Architecture**

The Ground station part is responsible for mission planning and uploading the mission to the airborne system. The operator using the Ground station can set the following parameters: starting point and endpoint of the mission at the ortophotomap or using the latitude and longitude coordinates, the altitude and velocity of the flight, the SAR radar head parameters as bandwidth and pulse repetition frequency, emitted power, SAR processing modes – focused/unfocused, the antenna beamwidth in elevation and azimuth and the inclination angle, the number of waypoints that can be determined automatically or manually. For the planned trajectory and each waypoint, the ground station cuts out an optical image region and then processes it to obtain the characteristic points. For this purpose, the ASIFT method is used, or the Sobel edge detection algorithm. The resulting optical image characteristic points for each waypoint are then uploaded to the airborne navigation-aid subsystem together with other essential parameters of the mission.

When the mission starts, the airborne system produces a given waypoint SAR image, and then the image is geotagged with the GPS/INS data (which might be incorrect). Then the image is processed, and the characteristic points are detected on the SAR image. Detected points on the SAR image and optical image are combined using the CMSD method, and the final latitude, longitude, and rotation correction are estimated. At that point, the main navigation system can use the correction estimation.

## 2.0 PROPOSED SOLUTION

The proposed solution is focused only on processing SAR imagery. The obtained SAR image is used to estimate rotation, longitude and latitude shift, and altitude information from the first strong reflection in the SAR image. The physical configuration of the SAR head allows for the observation and scanning of the ground and obtaining an altitude profile of the scanned area. Such configuration of operation is presented in Figure 1-2.

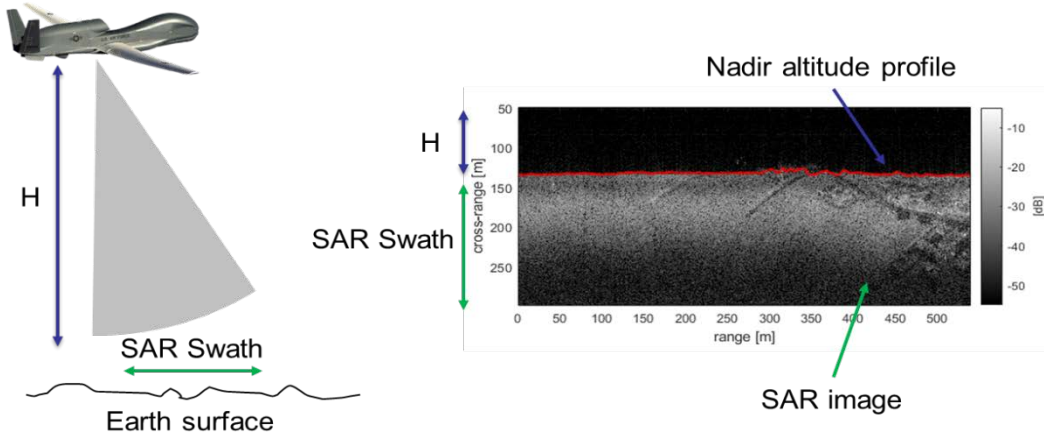


Figure 1-2: Implemented solution.

The SAR image is obtained at waypoints whose location is planned before the mission using the Ground station. The SAR image is then preprocessed to reduce speckle noise before the application of algorithms for characteristic point selection, such as Sobel edge detection or ASIFT algorithm [11]. The reduction of speckle noise is obtained by applying filters such as gamma-map, Lee, enhanced Lee, as well as multilook processing (but here, the degradation of the resolution in cross-range direction is observed).

## 2.1 Cumulative Minimum Square Distance Matching

The SAR image and the ground optical image stored in the database, both consist of pixels. Each pixel has its latitude and longitude coordinates assigned. In the case of optical images, it is assumed that their coordinates are correct. The internal GPS/INS system also geotags pixels from the SAR image. Such an internal system might be spoofed or jammed or just characterized by the accumulated time drifts. In such cases, the SAR image pixels geotagging is incorrect. To estimate the shift in longitude and latitude, and also the rotation of SAR image, we search for the minimum of the following expression:

$$\Omega(\Delta_{lat}, \Delta_{lon}, \alpha) = \sum_{n=0}^{N-1} \left\| R_{\alpha} \left( \vec{s}_n + \begin{bmatrix} \Delta_{lat} \\ \Delta_{lon} \end{bmatrix} \right) - \Psi \left( \Theta_{\sigma}, R_{\alpha} \left( \vec{s}_n + \begin{bmatrix} \Delta_{lat} \\ \Delta_{lon} \end{bmatrix} \right) \right) \right\|_2, \quad (1)$$

where  $\Delta_{lat}$  and  $\Delta_{lon}$  are the latitude and longitude errors in meters, respectively,  $\alpha$  stands for the rotation angle,  $\vec{s}_n$  is a two-dimensional vector in meters representing the n-th point of total N points extracted from the SAR image,  $\Theta_{\sigma}$  is the corresponding set of vectors representing points extracted from the optical image.  $\Psi$  is a function which returns vector  $\vec{v}$  from a set  $\mathcal{V}$  minimizing the distance to a given vector  $\vec{x}$ . The function  $\Psi$  is defined as follows:

$$\Psi(\mathcal{V}, \vec{x}) \triangleq \underset{\vec{v} \in \mathcal{V}}{\operatorname{argmin}} \|\vec{x} - \vec{v}\|_2. \quad (2)$$

The function  $R_{\alpha}$  is a rotation of two-dimensional vector  $\vec{x}$ , around point  $\vec{s}$ :

$$R_{\alpha}(\vec{x}) \triangleq (\vec{x} - \vec{s}) \cdot \begin{bmatrix} \cos \alpha & -\sin \alpha \\ \sin \alpha & \cos \alpha \end{bmatrix} + \vec{s}, \quad (3)$$

where  $\bar{s}$  stands for the mean value of all points extracted from the SAR image  $\vec{s}_m$ :

$$\bar{s} = \frac{1}{N} \sum_{m=0}^{N-1} \vec{s}_m \quad (4)$$

## 2.2 Altitude Measurement

Longitude and latitude shifts can only be correctly estimated if the platform altitude is known. Moreover, the instantaneous altitude is needed to transform the SAR image from slant-range to ground-range correctly. As mentioned earlier, the presented system allows for altitude estimation based on the SAR image. If the system utilizes other altitude sensors, the estimated value can be used to enhance the measurement precision. A simultaneous SAR imaging and altitude measurement concept is presented in Figure 1-2. In this scenario, the nadir signal is visible in the SAR image, however, only a part of the SAR image is being used for the horizontal trajectory error estimation.

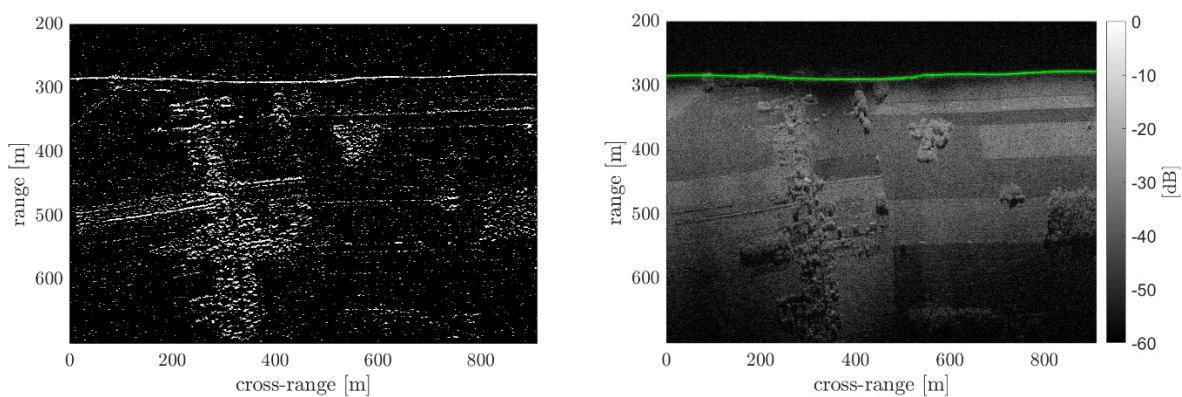


**Figure 2-1: Nadir signal detection, CA-CACFAR detection map (left), SAR image with nadir reflection indicated (right).**

The  $w$  is based on nadir signal detection. For this purpose, the cell averaging constant false alarm ratio detection (CA-CFAR) is used. CFAR detection map and corresponding SAR image are presented in Figure 2-1. Morphological image operations are applied to the detection map to clear unwanted false-alarm detections at low ranges. If the terrain can be considered as a flat, horizontal plane, the remaining continuous line indicates the closest strong nadir reflection coming from the ground directly below the platform. The nadir reflection has been indicated in Figure 2-1 with a green curve.

In Figure 2-2, the altitude calculated from the range of the nadir signal is presented. The GPS altitude, as well as altitude resulting from onboard atmospheric pressure measurements, are shown for comparison. As it can be seen, the radar measurement is consistent with the other two. Minor differences (often less than 1m) can result from the varying terrain height profile or the specific way the navigational platform processes the data (e.g., data smoothing, Kalman filtering).



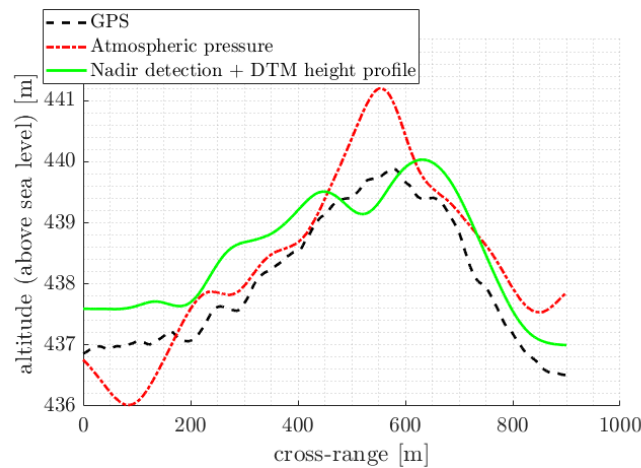


Figure 2-2: GPS, barometric formula, and nadir detection-based altitude measurement comparison.

### 3.0 RESULTS

In this section, the authors present the results of processing real-life data. For the real-life SAR images, the latitude, longitude and rotation error was introduced to geoinformation which allowed the algorithm validation under controlled conditions.

#### 3.1 Real-life data

The real-life data was acquired during the measurement campaign conducted in June 2021 in Płock, Poland. The radar demonstrator was mounted on the Cessna aircraft as shown in Figure 3-1. The parameters of the radar were as follows: carrier frequency: 10 GHz, signal bandwidth: 0.5 GHz, sweep repetition rate: 2 kHz. The radar was flying at the altitude of 1000 m with a velocity 40 m/s.

The optical image and the corresponding SAR image with the characteristic points detected using the edge detector and the ASIFT method are illustrated in Figure 3-2. The points were found on the industrial infrastructure which allows for creation of characteristic structures along e.g., pipes or buildings. The assumptions on image size, overlap and admissible error were the same as in the pseudo SAR case. The real-life SAR image geoinformation was manually disturbed according to Table 3-1. The results of the processing for the CMSDM and for the ASIFT-ICP methods are listed in Tables 3-2 and 3-3, respectively.

Table 3-1: Simulated navigation errors.

No.	Longitude error [m]	Latitude error [m]	Rotation [°]
1.	-8	5	1
2.	12	-8	1.5
3.	-25	-23	-2
4.	48	-31	2.5
5.	-59	40	-3
6.	80	50	4

**Table 3-2: Estimated navigation errors for the real-life image using the joint CMSDM method.**

No.	Estimated longitude error [m]	Estimated latitude error [m]	Estimated rotation error [°]	Processing time [s]
1.	-7.81	5.62	1.26	107
2.	11.82	-6.97	1.77	124
3.	-26.48	-24.21	-1.73	198
4.	49.31	-29.17	2.53	204
5.	-60.74	38.33	-2.93	136
6.	82.18	52.70	3.93	182

**Table 3-3: Estimated navigation errors for the real-life image using the joint ASIFT-ICP method.**

No.	Estimated longitude error [m]	Estimated latitude error [m]	Estimated rotation error [°]	Processing time [s]
1.	6.75	-1.75	2.19	1052
2.	5.25	-13.25	-2.21	1130
3.	-0.70	-11.85	-0.83	1.125
4.	10.75	-35.50	-2.99	1128
5.	3.25	-5.75	-.204	1.157
6.	8.85	14.25	-1.39	1219

As it can be seen, in the proposed method the estimation error is out of the assumed range ( $\pm 2$  m and  $\pm 0.5^\circ$ ) only for the last case characterized by the highest shift and rotation drift. However, the discrepancy between the assumed possible estimation error and the estimated one is negligible and equals 18 cm for the longitude and 70 cm for the latitude. Apart from these slight differences for case no. 6 (whose errors can be ignored), the method works correctly for real-life data. The outcomes are comparable to the ones obtained using the state-of-the-art technique, namely joint ASIFT-ICP method. It is apparent, that the methods failed and none of the cases gave an appropriate estimate. Also, the processing time is significantly higher, i.e. it is 5~10 times longer. The results clearly show that the CMSDM algorithm works faster and with an improved precision when compared to the method from the literature. The sample point distribution before and after correction for the methods in question is presented in Figure 3-3. As it can be seen, method proposed by the authors of this article works well even for the largest error (no. 6).

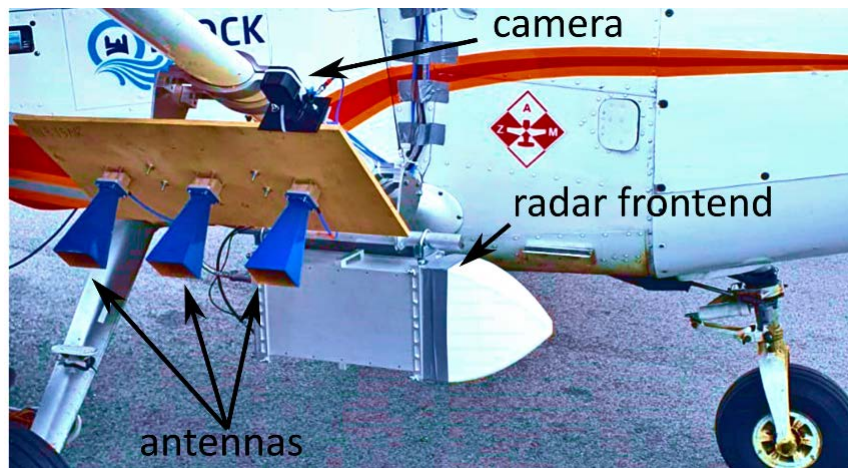


Figure 3-1: X-band radar sensor mounted on the Cessna aircraft.

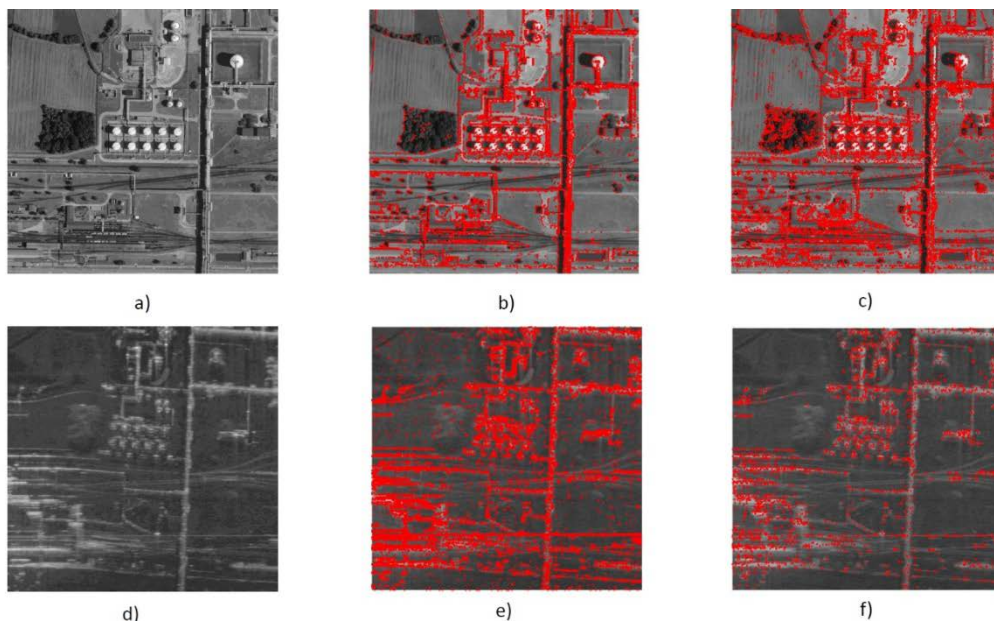
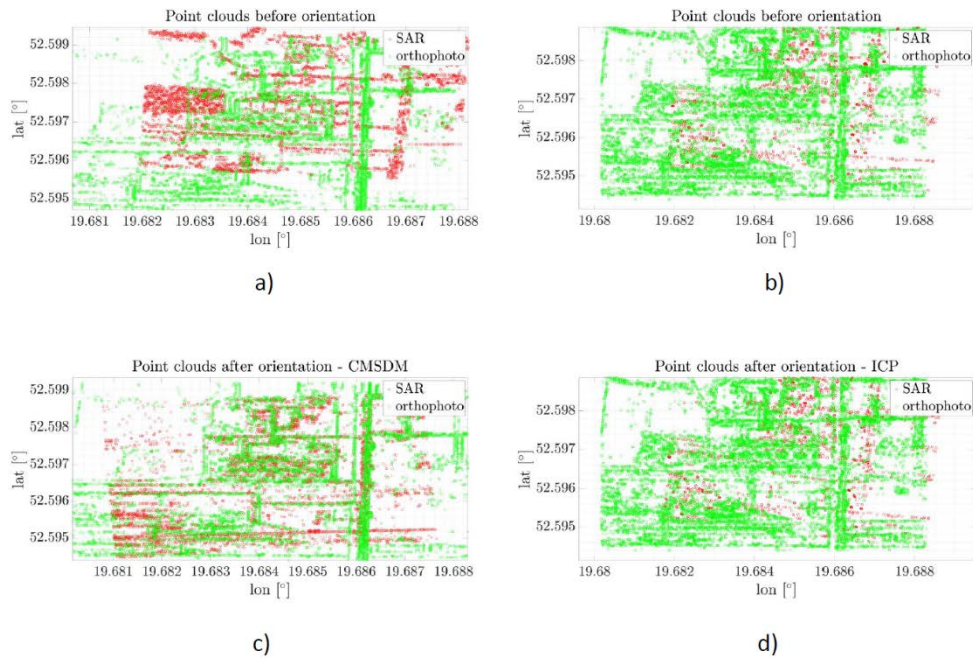


Figure 3-2: Processed images and the points detected on them. a) Optical image; b) Points detected on the optical image using the edge detector; c) Points detected on the optical image using the ASIFT algorithm; d) Real-life SAR image; e) Points detected on the real-life SAR image using the edge detector; f) Points detected on the real-life SAR image using the ASIFT algorithm.





**Figure 3-3: Point clouds before and after orientation using two methods under investigation. Example for the error no. 6. Red points -- SAR image, green points -- optical image a) Point clouds extracted using the edge detector before orientation; b) Point clouds extracted using the ASIFT algorithm before orientation; c) Point clouds after matching using CMSDM; d) Point clouds after matching using ICP.**

## 4.0 CONCLUSIONS

This paper presents a novel technique that aims to improve navigation guidance when a flying platform lacks a GPS/GNSS signal, or when the signal is present but jammed. As presented in this paper, the proposed solution allows one to obtain high precision (below 2 m) significantly faster than the method known from the literature. The developed algorithm was tested and validated using real-life measurements. The subsequent experiment showed the superiority of the CMSDM algorithm over the combined ASIFT-ICP method that serves as the reference in this work. It is worth mentioning that the proposed method works for totally different images, namely SAR and optical. To the author's knowledge, the problem of matching two images of a different nature is of interest. Plans for the future include a real-time implementation of the proposed CMSDM on a flying platform for online error estimation.

## REFERENCES

- [1] Golden, P. J. Terrain contour matching (TERCOM): A cruise missile guidance aid. *Image Process. Missile Guid.* 1980, 238, 10-18.
- [2] Vaman, D. TERRAIN REFERENCED NAVIGATION: History, trends and the unused potential. In Proceedings of the 31st Digital Avionics Systems, Williamsburg, VA, USA, 14–18 October 2012; pp. 1–28.
- [3] Hwang, Y.; Tahk, M.J. Terrain Referenced UAV Navigation With LIDAR—A Comparison of Sequential Processing and Batch Processing Algorithms. In Proceedings of the 28th International Congress of the Aeronautical Sciences, ISAC, Brisbane, Australia, 23–28 September 2012; pp. 1–7.
- [3] G. Franceschetti, R. Lanari, Synthetic Aperture Radar Processing, 1999 CRC Press LLC.
- [4] AI Haojun, HU Ruimin, DING Mingyue. A New Algorithm for DSMAC Simulation[J]. *Geomatics and Information Science of Wuhan University*, 2001, 26(3): 261-265.
- [5] "Image Processing For Tomahawk Scene Matching". Johns Hopkins APL Technical Digest, Volume 15, Number 3. Geoffrey B. Irani and James P. Christ.
- [6] Jon R. Carr and James S. Sobek "Digital Scene Matching Area Correlator (DSMAC)", Proc. SPIE 0238, Image Processing for Missile Guidance, (23 December 1980); <https://doi.org/10.1117/12.959130>
- [7] Greco, M.; Pineli, G.; Kulpa, K.; Samczyński, P.; Querry, B.; Querry, S. The study on SAR images exploitation for air platform navigation purposes, in Proc. of the International Radar Symposium (IRS 2011), September 7-9, 2011, Leipzig, Germany, pp. 347-352.
- [8] Greco, M.; Kulpa, K.; Pinelli, G.; Samczyński, P. SAR and InSAR georeferencing algorithms for Inertial Navigations Systems, Proc. of SPIE, vol. 8008 (SPIE, Bellingham, WA, 2011). pp. 8008 10 (20-23).
- [9] Greco, M.; Querry, S.; Pinelli, G.; Kulpa, K.; Samczyński, P.; Gromek, D.; Gromek, A.; Malanowski, M.; Querry, B.; Bonsignore, A. SAR-based Augmented Integrity Navigation Architecture, in Proc. on IRS 2012, 23-25 May 2012, Warsaw, Poland, pp. 225-229.
- [10] Abratkiewicz, K.; Gromek, D; Samczyński, P.; Markiewicz J.; Ostrowski, W. The Concept of Applying a SIFT Algorithm and Orthophotomaps in SAR-based Augmented Integrity Navigation Systems, 2019 20th International Radar Symposium (IRS), Ulm, Germany, 2019, pp. 1-12.
- [11] Yu, G.; Morel, J.-M. ASIFT: An Algorithm for Fully Affine Invariant Comparison. *Image Process. Line* 2011, 1, 11–38, doi:10.5201/ipol.2011.my-asift.